

Supporting Information

Gut microbiome perturbations induced by bacterial infection affect arsenic biotransformation

Kun Lu^{†,§,*}, Peter Hans Cable[#], Ryan Phillip Abo[‡], Hongyu Ru[§],
Michelle E. Graffam^{||}, Katherine Ann Schlieper^{||}, Nicola M.A. Parry^{||},
Stuart Levine^{†,‡}, Wanda M Bodnar[#], John S. Wishnok[†], Miroslav Styblo^{#,α},
James A Swenberg[#], James G. Fox^{†,||} and Steven R. Tannenbaum^{†, Δ}

†. Department of Biological Engineering; ‡. Department of Biology;
||. Division of Comparative Medicine; Δ. Department of Chemistry
Massachusetts Institute of Technology, Cambridge, Massachusetts, 02139, USA.
#. Department of Environmental Sciences and Engineering;
α. Department of Nutrition
University of North Carolina, Chapel Hill, NC, 27599, USA
§. Department of Environmental Health Science,
University of Georgia, Athens, GA, 30602

Table of Contents

Gut bacteria abundance at phylum level of each sample revealed by 16S rRNA sequencing (Figure S1)	S-2
Histological analysis for the controls and infected animals, with inflammation being scored for multiple regions of the colon and liver (Figure S2)	S-3
Correlation analysis between iAsV with methylated (DMAsV) and thiloated arsenic species (DMTAs) in 1 day-exposed samples (Figure S3)	S-4
The dynamic interaction between the gut microbiome perturbations and arsenic species (Figure S4).....	S-5

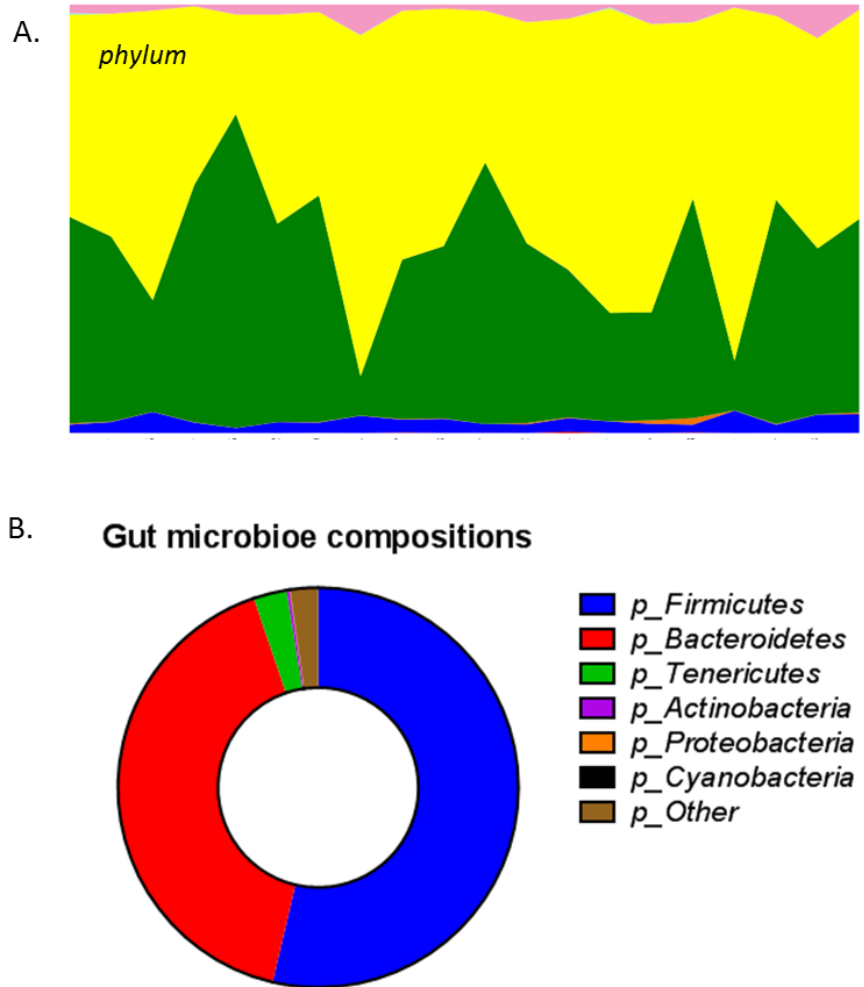


Figure S1. Gut bacteria abundance at phylum level of each sample revealed by 16S rRNA sequencing (each color represents one bacterial phylum) (A), with *Firmicutes* (~53.6%) and *Bacteroidetes* (~41.1%) being predominant, followed by *Tenericutes* (~2.7%), *Actinobacteria* (~0.2%), *Cyanobacteria* (~0.05%) and *Proteobacteria* (~0.02%), with 2.2% unassigned sequences (B).

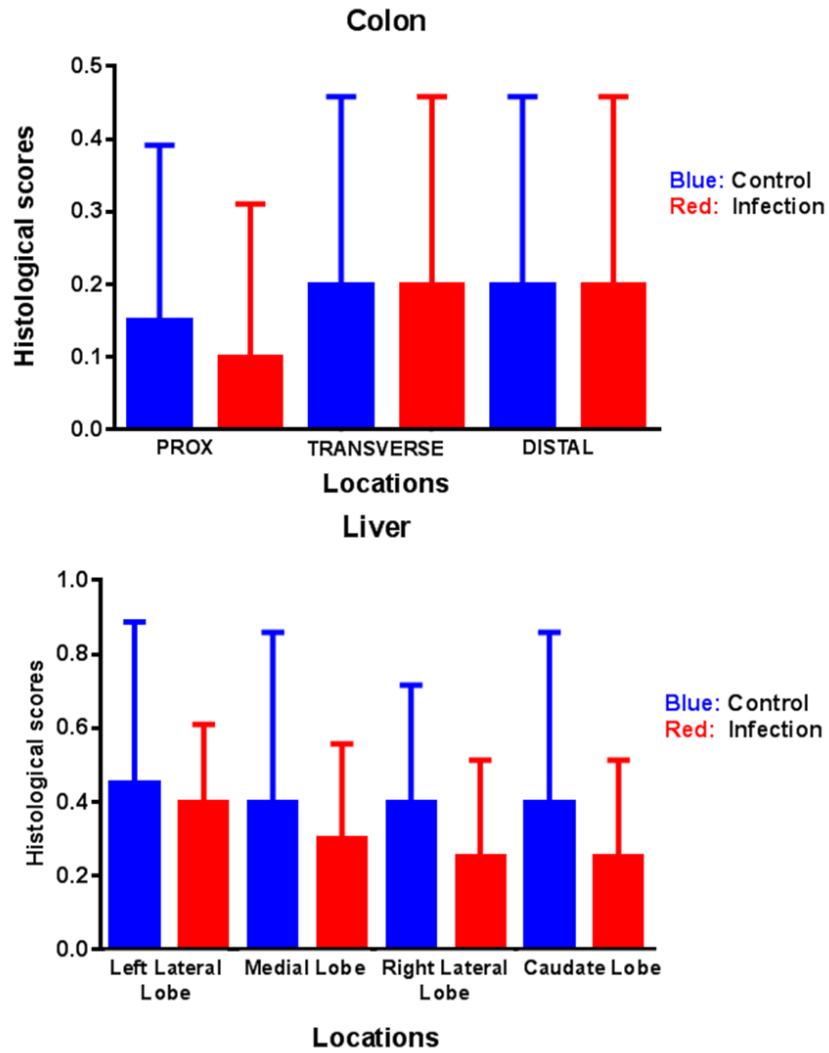


Figure S2. Histological analysis for the controls and infected animals, with inflammation being scored for multiple regions of the colon (A) and liver (B), with no statistically significant different being identified between the controls and infected animals. The scores for other endpoints, including edema, epithelial defects, crypt atrophy, hyperplasia and dysplasia, are generally normal.

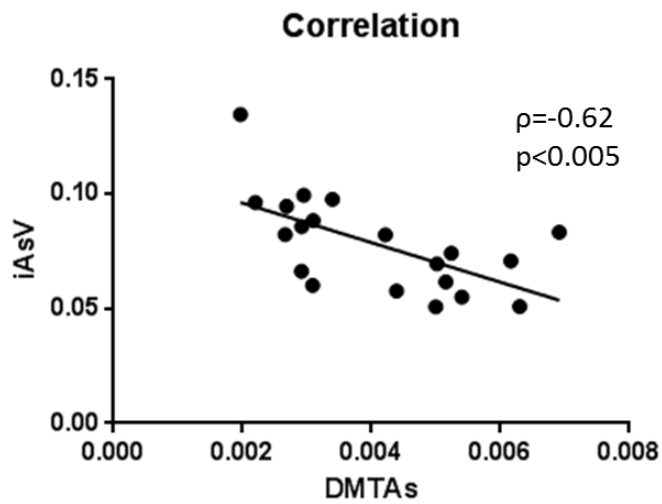
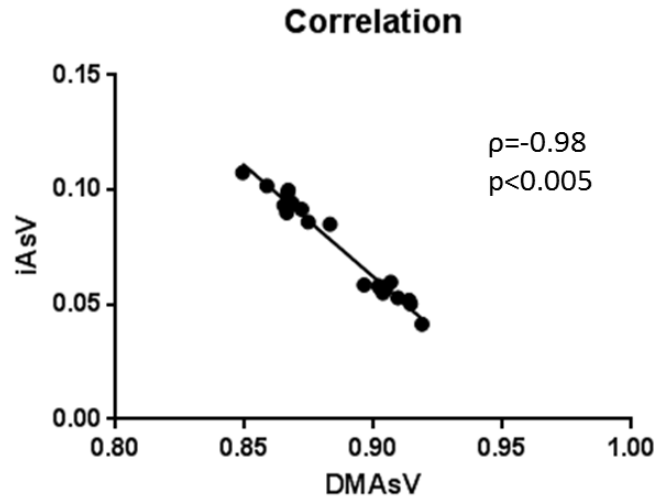


Figure S3. Correlation analysis between iAsV with methylated (DMAsV) and thiolated arsenic species (DMTAs) in 1 day-exposed samples, as determined by Pearson's correlation coefficient. IAsV was negatively correlated with both methylated (DMAsV) and thiolated (DMTAs) arsenic species ($\rho < -0.5$ and $p < 0.05$).

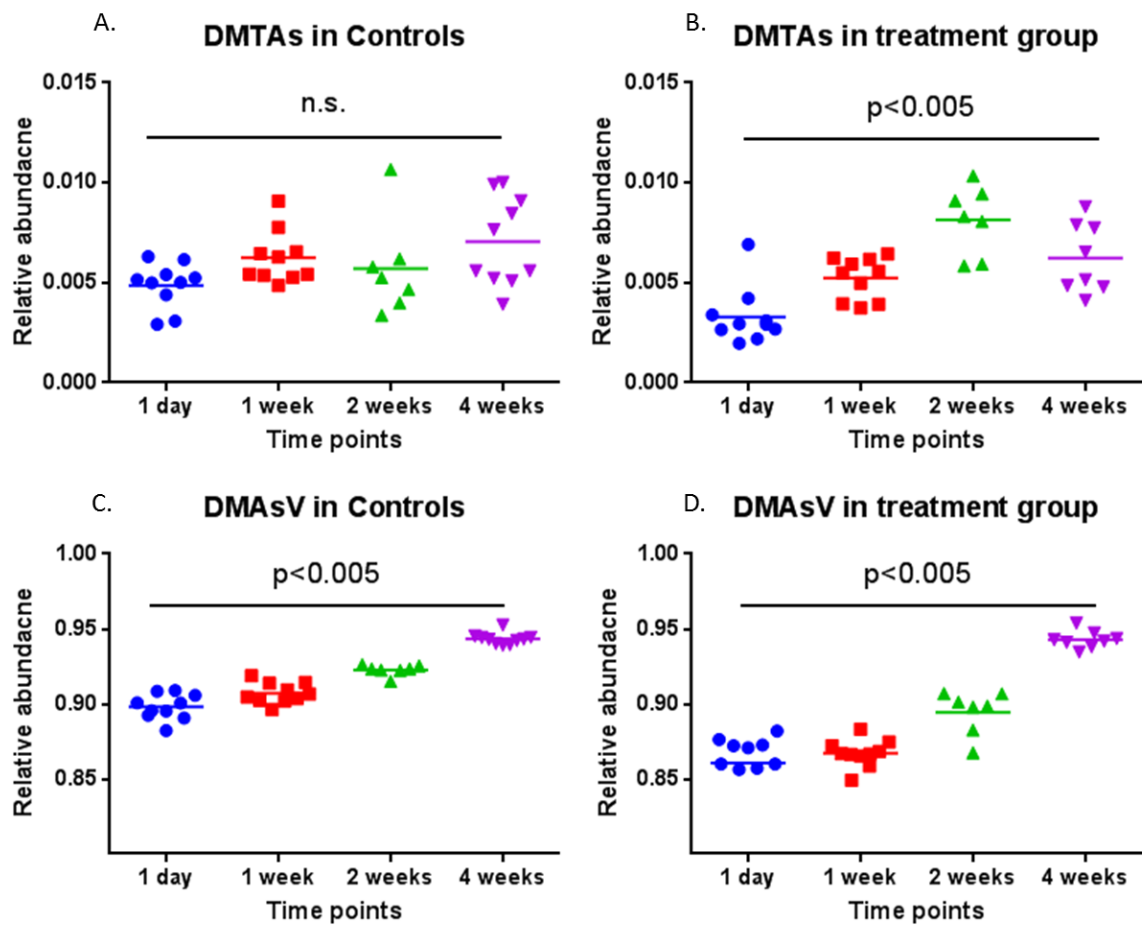


Figure S4. The dynamic interaction between the gut microbiome perturbations and arsenic species: DMTAsV, a gut-flora-generated thiolated arsenic species (A and B), and DMAsV, a methylated arsenic metabolite during the detoxification pathway of inorganic arsenics (C and D).